Springer

Journal of Mechanical Science and Technology 23 (2009) 409~419

Journal of Mechanical Science and Technology

www.springerlink.com/content/1738-494x
DOI 10.1007/s12206-008-1103-4

Mapping of the morphological and the material characteristics on the glenoid and estimation of predominant loading condition on the glenoid through the mapping †

Dohyung Lim[1,2], Han-Sung Kim[3], Jung-Sung Kim[4,5], Rami Seliktar[1] and Sung-Jae Lee[6,*]

[1]*School of Biomedical Engineering, Science and Health Systems, Drexel University, Pennsylvania 19104, United States*
[2]*Silver Technology Center, Korea Institute of Industrial Technology, Chungnam, 330-825, Korea*
[3]*Department of Biomedical Engineering, Yonsei University, Gangwon 220-710, Korea*
[4]*Department of Medical Engineering, Yonsei University College of Medicine, Seoul, 120-752, Korea*
[5]*BK 21 Project for Medical Science, Yonsei University College of Medicine, Seoul, 120-752, Korea*
[6]*Department of Biomedical Engineering, Inje University, Gyoungnam, 621-749, Korea*

(Manuscript Received October 11, 2007; Revised June 3, 2008; Accepted November 11, 2008)

Abstract

The aim of this study was to predict and map the regional distribution of the trabecular architecture and the material properties of the glenoid and to estimate the predominant loading condition on the glenoid through the mapping. The morphological and material characteristics of the glenoid were investigated by analyzing digitized trabecular bone images obtained from twelve cadaver scapula specimens. The morphological and material characteristics computed from the cadaver specimens show that the predominant loading on the glenoid generally occurs during shoulder movement, which produces forces directed toward the posterior aspect of the bare region. This study is innovative in its detailed mapping of the morphological and material characteristics of the glenoid and its pioneering approach used to estimate the loading pattern acting on the glenoid through the mapping.

Keywords: Trabecular architecture; Material property; Glenoid; Glenohumeral joint; Predominant loading condition

1. Introduction

To date, numerous studies have investigated the material, mechanics, and morphology of cancellous bone [1-23]. Understanding the relationships between these characteristics in cancellous bone can provide information for determining the risk of bone fracture and for planning surgical procedures and rehabilitation protocols in individuals with musculoskeletal pathologies, particularly in the shoulder joint. Musculoskeletal pathologies influence the material, mechanics, and morphology of cancellous bone by altering the loading conditions. The ability to predict the degree of change in these characteristics should reduce the likelihood of the failure of prosthetic implants. However, unlike other anatomical regions, the glenoid has been the focus of relatively few studies of material and morphological characteristics with consideration of the functional activities of the shoulder. Since the shoulder joint has a complex anatomy and mobility, few studies have been performed compared to the other skeletal joints.

In the second half of the 19th century, von Meyer [24] and Wolff [25] observed that cancellous bone has "a well-motivated architecture, which is closely related to its statics and mechanics" and suggested that trabeculae align themselves along stress trajectories, *i.e.*, the directions in which only pure compressive or tensile stress occur [26]. More recently, Goldstein et al. [5], Guldberg et al. [6],

† This paper was recommended for publication in revised form by Associate Editor Young Eun Kim

*Corresponding author. Tel.: +82 55 320 3452, Fax.: +82 33 320 3452.
E-mail address: sjl@bme.inje.ac.kr / dli349@gmail.com

Tsubota et al. [16], Miller et al. [10], Huiskes et al. [8], and van Rietbergen et al. [20] attempted to quantify Wolff's Law by correlating the relationship between morphology (trabecular architecture) and mechanics (loading and boundary conditions) by using a finite element method (FEM) or in vivo experimental test. They illustrated the predicted trabecular bone adaptation under various mechanical conditions through FEM and confirmed that remodeling of the trabecular architecture is governed by the mechanical conditions acting on bone through in vivo experimental test. These studies offer a clue to understanding the mechanics of the glenoid and indicate that the predominant loading condition corresponding to the material and morphological characteristics may be estimated.

The aim of the current study was to map in detail the morphological and material characteristics of the glenoid and to estimate the predominant loading condition acting on the glenoid through the mapping using the relationship between the mechanics and the morphology and material. The information may be basically significant for studying the mechanical behavior of the glenoid and to understanding of a variety of pathological shoulder conditions. It also may be applicable to related orthopedic implants and therapies.

2. Materials and methods

2.1 Preparation of cadaver specimens

After examination of the existence of any bone or muscle pathology, twelve cadaver scapulae (all from people more than 60 years old) were used to determine the trabecular architecture and material properties of cancellous bone in the glenoid. The cadaver scapulae were harvested, and the glenoid was sliced into 2-mm slices. Each section of sliced bone was treated to remove the extracellular matrix (ECM: marrow) in order to enhance the trabeculae and was digitized (640 × 480 pixels) at a resolution of 35 μm. Six regions of interest (ROIs, 100 × 100 pixels in each ROI) were assigned on each sliced bone (Fig. 1). The selection of the ROIs on the digitized images and the size of each ROI were determined by the intrinsic geometry of the glenoid [27-30]. The distributions and sizes of the ROIs considered in the current study covered the entire region of the glenoid for analysis of the morphological and mechanical characteristics of the entire glenoid, as established previously [27-30].

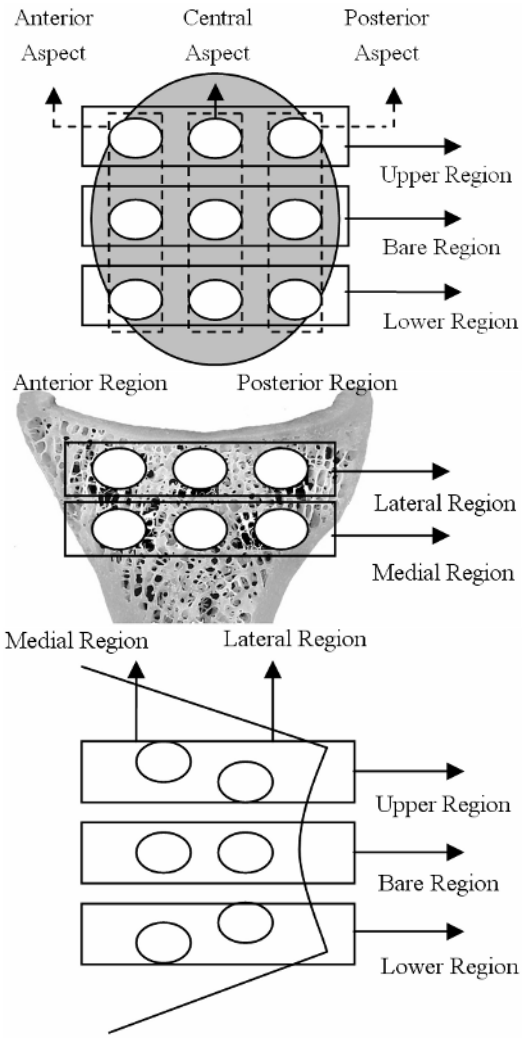

Fig. 1. Schematic of the locations of the regions of interest (ROIs) in the mediolateral (above), supero-inferior (center), and anteroposterior (bottom) views.

Vertically, the glenoid was divided into three regions: the upper, bare (the area of maximum concavity of the glenoid joint surface), and lower regions. Each of the three regions was seen in several slices, depending on the individual specimen. The different images of a particular region were analyzed and averaged for that region. This procedure produced a total of 18 regions (6 ROIs × 3 regions) representing the six ROIs in the upper, bare, and lower regions (Fig. 1).

2.2 Measuring trabecular architecture

Mean Intercept Length (MIL): The mean intercept length (MIL) was measured for each ROI in the

digitized images of the glenoid. The basic principle of MIL measurement is to count the number of intersections between a linear grid and the trabeculae/marrow interface as a function of the grid orientation ω; see Fig. 2 [3, 12]. The MIL, or mean length between two intersections, is defined conceptually as the total line length (L) divided by the number of intersections (I) in angle ω (refer to Eq. 1) [3, 12].

$$MIL_p = 2 \times V_v(p) \frac{L}{I(\varpi)} \tag{1}$$

where p: the phase of interest (bone or marrow), $V_v(p)$: the volume fraction, L: the total line length, I: the number of intersections, and ω: the angle of the grid line.

The MIL value was obtained by using Eq. (1). For the three-dimensional analysis, it was assumed that cancellous bone in the transverse plane is transversely isotropic, which implies that the MIL obtained in the anteroposterior direction should be the same as that in the superoinferior direction. These MILs were calculated for all of the ROIs using grids from 0 to 165°, at 15°-intervals. A factor of 2 was used in Eq. (1) because 2 × MIL is the mean length of the bone + marrow intercept.

Predominant Trabecular Direction (Angle): The MIL obtained for each ROI was fitted to an ellipse to calculate the fabric tensor ***H***. The eigenvalues (MIL in the principal axes) and eigenvector (direction of the principal axes) of ***H*** were calculated as described in the literature [2, 3, 9, 13, 14, 17, 18, 31]. The eigenvector was then used to determine the primary principal axis of the trabeculae in each ROI. Finally, the predominant trabecular direction (angle) for each ROI was quantified by using the angle between the glenoid articular surface axis and the primary principal axis (Fig. 3).

2.3 Calculating material characteristics

In the analysis of the material properties of the glenoid, the degree of anisotropy and elastic tensor were calculated. The degree of anisotropy and elastic tensor were computed from the sliced bone images of the cadaver specimens assuming that the glenoid is transversely isotropic [3, 27, 28-30]. All these parameters were computed for the ROIs defined in the measurement of trabecular architecture.

The normalized eigenvalues ($\lambda_i = e_i/\Sigma e_i$, $\lambda_1 + \lambda_2 + \lambda_3 = 1$) calculated from ***H*** were used to quantify the degree of anisotropy. Although ***H*** itself may be used to represent the degree of anisotropy [18], the anisotropy index is more convenient for understanding the overall mechanical and morphological characteristics of the glenoid. The anisotropy index was determined from second invariant terms ($\Pi = \lambda_1\lambda_2 + \lambda_2\lambda_3 + \lambda_3\lambda_1$).

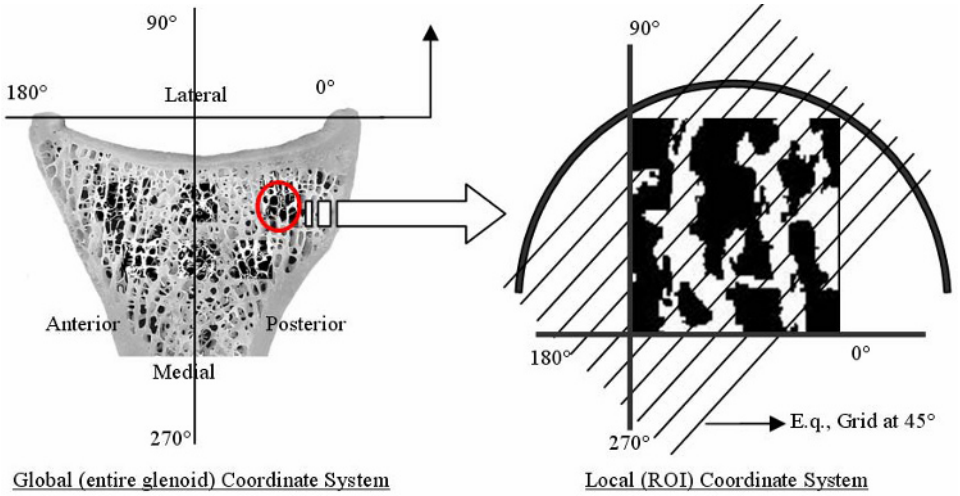

Fig. 2. Method for calculating the mean intercept length (MIL). Here, the grid for calculating the MIL is selected at 45° on an ROI chosen from a sliced bone image. The global coordinate system is placed on the center of the glenoid articular surface, and the local coordinate is located at the lower-left edge of each ROI. The horizontal axis in the local coordinate system parallels that of the global coordinate system.

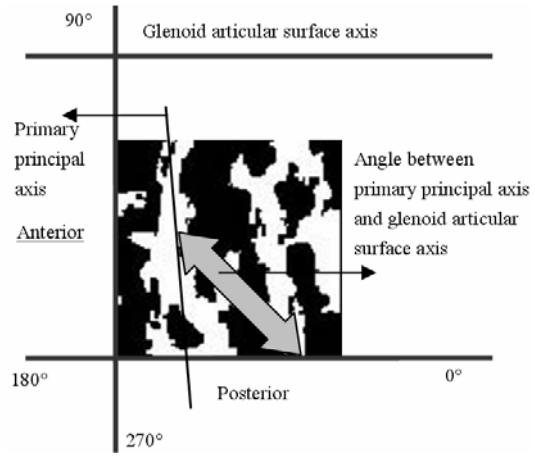

Fig. 3. Method for calculating the angle between the primary glenoid axis and the glenoid articular surface axis. The glenoid articular surface axis on each ROI is defined by the line parallel to the horizontal axis of the global coordinate system.

The minimum value corresponds to a unidirectional fabric ($\lambda_1 = 1$, $\lambda_2 = \lambda_3 = 0$), and the maximum value corresponds to isotropic material ($\lambda_1 = \lambda_2 = \lambda_3 = 1/3$). Intermediate values of Π represent intermediate degrees of anisotropy. The elastic tensor was calculated from the elastic constant and the fabric tensor $\boldsymbol{H}$ (Eqs. 2-4) by using a simplified relationship suggested by Turner and Cowin [17] that normalizes the fabric tensor eigenvalues requirement at $H_1 + H_2 + H_3 = 1$ [32, 17, 33].

$$C_{iiii} = E_t[k_1 + 2k_6 + (k_2 + 2k_7)\Pi + 2(k_3 + 2k_8)\lambda_i + (2k_4 + k_5 + 4k_6)\lambda_i^2] \quad (2)$$

$$C_{iijj} = E_t[k_1 + 2k_2\Pi + k_3(\lambda_i + \lambda_j) + k_4(\lambda_i^2 + \lambda_j^2) + k_5\lambda_i\lambda_j] \quad (3)$$

$$C_{ijij} = E_t[k_6 + k_7\Pi + k_8(\lambda_i + \lambda_j) + k_9(\lambda_i^2 + \lambda_j^2)] \quad (4)$$

where E_t: the tissue modulus, λ_i and λ_j: the fabric tensor, $i, j = 1, 2, 3$ and $i \neq j$, $\Pi = \lambda_1\lambda_2 + \lambda_2\lambda_3 + \lambda_3\lambda_1$, and k_1-k_9: constants that are a function of the volume fraction (apparent density).

Here, k_1-k_9 are obtained from:

$$k_m(\nu_\nu) = k_{ma} + k_{mb}\nu_\nu^p \quad (5)$$

where $m = 1, 2, \ldots, 9$, $p = 1.6$, and ν_ν: volume fraction (apparent density).

After reviewing various methods for determining constants k_1 through k_9 [3, 9, 15, 19, 31], we adopted the constants reported by Kabel et al. [9]. We assumed that k_1-k_9 can be used for cancellous bone in general because the constants determined by Kabel et al. [9] are based on the largest range of ages and numbers of observations [9, 31]. Finally, the apparent density was applied to Eqs. (2-4) to calculate the elastic tensor in each ROI. In Eqs. (2-4), E_t = 1 GPa [9, 19]. The results calculated by using E_t = 1 GPa can be scaled subsequently by applying other values of the tissue modulus to Eqs. (2-4).

3. Results

On examining the cadaver specimens, no significant pathologies were seen.

3.1 Characteristics of trabecular architecture

Regional Variation in the Mean Intercept Length: The respective values of the MIL obtained for the primary and secondary principal axes were 0.42 ± 0.07 and 0.30 ± 0.06 mm for the upper region, 0.44 ± 0.08 and 0.30 ± 0.06 mm for the bare region, and 0.43 ± 0.07 and 0.30 ± 0.06 mm for the lower region. Figure 4 shows the complete distribution of the MIL values for the 18 regions, along the primary and secondary principal axes. The MILs in the primary principal axis for the posterior region are generally higher than those for the other regions. The MILs in the secondary principal axis are similar for all 18 regions, unlike the MILs in the primary principal axis. The difference (0.18 ± 0.03 mm, maximum) in length between the MILs (0.46 ± 0.05 mm, maximum) in the primary principal axis and the MILs (0.28 ± 0.04 mm, maximum) in the secondary principal axis for the posterior region was greater than the difference for the other regions of the glenoid. This indicates that the posterior region is very anisotropic and that the trabeculae in this region are better adapted to loading conditions than are those in other regions. The MILs calculated for each ROI of the glenoid show a peak in the range of 75 to 120° relative to the glenoid articular surface axis (Fig. 5). This indicates that the load distributed on the glenoid articular surface is greatest at the center of the glenoid.

Predominant Trabecular Direction (Angle): The predominant trabecular direction (angle) was 89.4 ± 10.1° when the entire glenoid was considered as a single region. The predominant trabecular direction in

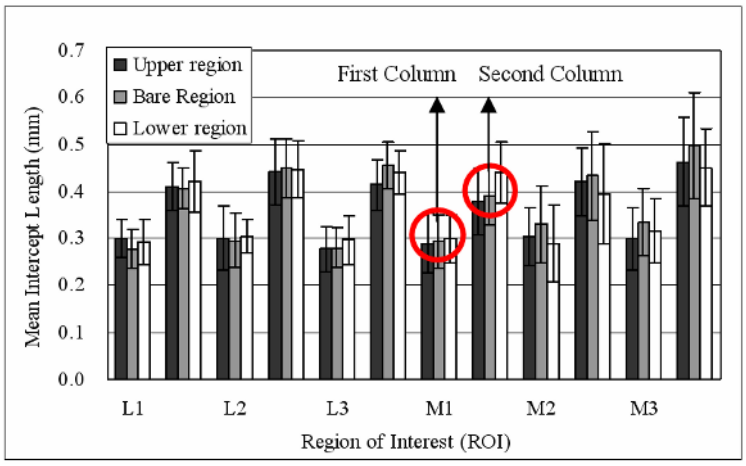

Fig. 4. MIL in the primary and secondary axes for the entire glenoid (L: lateral, M: medial, 1: anterior, 2: center, 3: posterior). The first and second columns for each ROI indicate the MIL in the secondary and primary axes, respectively.

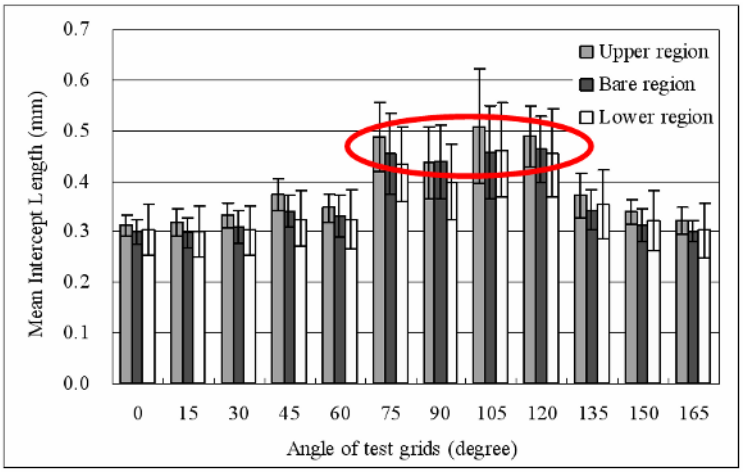

Fig. 5. An example of the MIL distribution on an ROI located in the posterior portion of the glenoid, with the change in grid angle. The MILs in the ellipse are all higher than those at other angles.

each region is shown in detail in Fig. 6. The directions in all of the ROIs are nearly perpendicular to the glenoid articular surface axis. The predominant trabecular direction in the anterior portion (95.4 ± 9.5°, directed anteriorly) of the lateral region is oriented rather anteriorly relative to the glenoid articular surface axis compared with that in the central (87.9 ± 7.7°, directed posteriorly) and posterior (89.8 ± 7.3°, directed posteriorly) portions of the lateral region.

The predominant trabecular directions in the anterior, central, and posterior portions of the medial region are 92.8 ± 12.5° (directed anteriorly), 86.0 ± 10.0° (directed posteriorly), and 84.7 ± 8.8° (directed posteriorly), respectively. These results were obtained when the entire glenoid was classified into three broad regions, the anterior, central, and posterior regions. The predominant trabecular directions in the upper, bare, and lower regions were 89.4 ± 10.1°, 89.3 ± 10.6°, and 89.6 ± 9.6°, respectively, indicating that the glenoid is subjected to loading that is predominantly directed perpendicular to the glenoid articular surface.

3.2 Material characteristics of glenoid

Regional Variation of Degree of Anisotropy: The

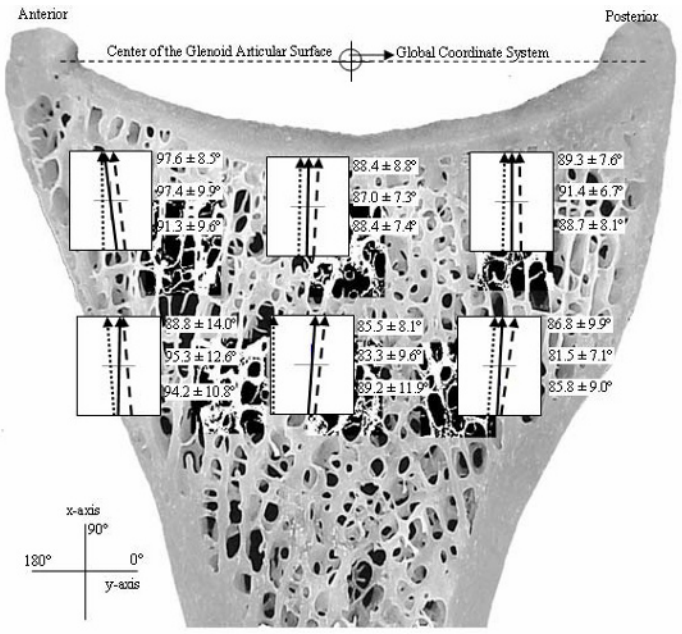

Fig. 6. Predominant trabecular directions (average angle) and their distributions (standard deviation) in the ROIs. Straight, dashed, and dotted lines represent the predominant directions, in the upper, bare, and lower regions, respectively. The values in the first, second, and third rows in the ROIs are the predominant numerical angles in the upper, bare, and lower regions, respectively.

degree of anisotropy was 0.327 ± 0.003 when considering the entire glenoid as a single region. The corresponding reference value for exact isotropic behavior is 0.333. The glenoid in this section is not very anisotropic when considered as one region--it is close to isotropic. The degree of anisotropy is generally larger in the posterior than in the anterior or central regions. The degree of anisotropy in the lateral region of the glenoid is higher than that in the medial region.

Regional Variation of Elastic Tensor: The elastic tensor (units: MPa) calculated over the entire glenoid was:

$$\begin{bmatrix} 131\pm24 & 54\pm10 & 46\pm8 & 0 & 0 & 0 \\ 54\pm10 & 312\pm82 & 54\pm10 & 0 & 0 & 0 \\ 46\pm8 & 54\pm10 & 131\pm24 & 0 & 0 & 0 \\ 0 & 0 & 0 & 64\pm12 & 0 & 0 \\ 0 & 0 & 0 & 0 & 47\pm9 & 0 \\ 0 & 0 & 0 & 0 & 0 & 64\pm12 \end{bmatrix}$$

The following are the elastic tensors (units: MPa) for three broad regions of the glenoid, the upper, bare, and lower regions:

Upper region

$$\begin{bmatrix} 127\pm25 & 52\pm10 & 44\pm8 & 0 & 0 & 0 \\ 52\pm10 & 296\pm81 & 52\pm10 & 0 & 0 & 0 \\ 44\pm8 & 52\pm10 & 127\pm25 & 0 & 0 & 0 \\ 0 & 0 & 0 & 62\pm12 & 0 & 0 \\ 0 & 0 & 0 & 0 & 45\pm9 & 0 \\ 0 & 0 & 0 & 0 & 0 & 62\pm12 \end{bmatrix}$$

Bare region

$$\begin{bmatrix} 135\pm32 & 56\pm13 & 47\pm11 & 0 & 0 & 0 \\ 56\pm13 & 332\pm109 & 56\pm13 & 0 & 0 & 0 \\ 47\pm11 & 56\pm13 & 135\pm32 & 0 & 0 & 0 \\ 0 & 0 & 0 & 66\pm16 & 0 & 0 \\ 0 & 0 & 0 & 0 & 48\pm12 & 0 \\ 0 & 0 & 0 & 0 & 0 & 66\pm16 \end{bmatrix}$$

Lower region

$$\begin{bmatrix} 131\pm11 & 54\pm4 & 45\pm3 & 0 & 0 & 0 \\ 52\pm10 & 308\pm37 & 54\pm4 & 0 & 0 & 0 \\ 45\pm3 & 54\pm4 & 131\pm11 & 0 & 0 & 0 \\ 0 & 0 & 0 & 64\pm52 & 0 & 0 \\ 0 & 0 & 0 & 0 & 47\pm4 & 0 \\ 0 & 0 & 0 & 0 & 0 & 64\pm5 \end{bmatrix}$$

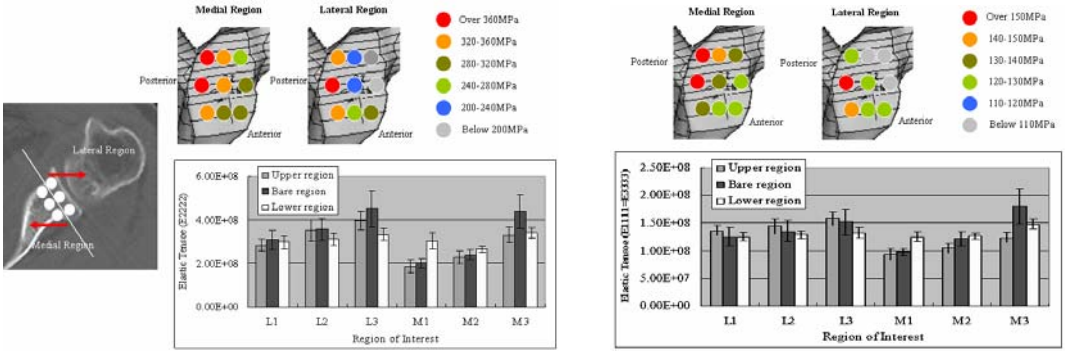

Fig. 7. Regional distribution of the elastic tensors (a) E_{2222}, (b) $E_{1111} = E_{3333}$, (c) E_{3311}, (d) $E_{1122} = E_{2233}$, (e) E_{3131}, (f) $E_{1212} = E_{3131}$ throughout the glenoid (L: lateral, M: medial, 1: anterior, 2: center, 3: posterior).

Although the elastic tensor values computed from the cadaver specimens are higher than the elastic modulus values calculated from the CT scans, the results compare more favorably with reported data than do the elastic modulus results [27-30]. This suggests that the elastic tensor calculated after considering both the trabecular architecture and the apparent density on the CT scans is more realistic than the elastic modulus calculated directly from the CT scan. The elastic tensors calculated in each ROI are shown in Fig. 7. The regional variation in the elastic tensor for the entire glenoid is similar to that of

the compressive strength and elastic modulus described above, suggesting that the load on the glenoid is as described in above.

4. Discussion and conclusions

The MIL method was used to determine the morphological and mechanical characteristics of the glenoid. The MIL method, which evaluates the planar trabecular alignment, can sometimes be a poor predictor of porous architecture [12]. However, Kabel et al. [9], van Lenthe and Huiskes [19], and others [3, 12] have reported that the MIL method performs slightly better than the volume-based methods (VO and SVD) in calculating the elastic tensor (mechanical characteristic) of cancellous bone, and the MIL method is sufficient to explain the trabecular architecture. The MIL method is also simpler than the volume-based methods. Therefore, we adopted the MIL method for the morphological analysis and for calculating the elastic tensor of the glenoid.

Little is known about the material properties of cancellous bone in the glenoid. Frich et al. [28] reported the topographic bone strength distribution as predicted by using the osteo-penetration test and elastic constants computed from the conventional *in vitro* compressive test. The strength at the proximal subchondral level of the glenoid averaged 66.0 MPa. High peak values were measured posterior, superior, and anterior to the area of maximum concavity of the glenoid joint surface. The average strength decreased by 25% at 1 mm below the subchondral plate and by 70% at 2 mm below it. The elastic modulus ranged from approximately 100 MPa for the bare area of the glenoid to 400 MPa in the superior part of the glenoid. Using the elastic constants to predict the mechanical anisotropy, the average anisotropy ratio was 5.2, indicating strong anisotropy. The apparent density averaged 0.35 g cm^{-3}, and the Poisson ratio averaged 0.263. Mansat et al. [30] measured the elastic properties of the glenoid bone in the axial, coronal, and sagittal planes using an ultrasound transmission technique. The relative density and CT numbers (in Hounsfield units) were also assessed. They found significant differences in the material properties at different anatomic locations. The material properties of cancellous bone were higher near the direction of application of the resultant force, perpendicular to the articular surface of the glenoid. The material properties were significantly higher at the center and posterior edge of the glenoid. Significant differences were also found in the three planes studied. The lateromedial Young's modulus (E_1 = 372 ± 164 MPa) was higher than the anteroposterior (E_2 = 222 ± 79 MPa) and superoinferior (E_3 = 198 ± 75 MPa) moduli. Using an indentation test, Anglin *et al*. [27] reported on the modulus and strength of glenoid cancellous bone in more detail, including regional variation. In that study, the measured mean strength of ten glenoid bones ranged from 6.7 to 17 MPa, with an overall mean of 10.3 MPa, and the mean elastic moduli ranged from 67 to 171 MPa for individual glenoid bones, with an overall mean of 99 MPa. They thought that these values were lower than those of normal bone because strength and modulus decrease with age and their specimens were from older subjects. They found that the strongest region was posterosuperior and that there was a large drop in strength and modulus below the subchondral layer.

The index of anisotropy (0.327 ± 0.003 for the entire glenoid) shows that the cancellous bone of the glenoid is close to isotropic. The corresponding reference value for exact isotropic behavior is 0.333. This supports the validity of the assumption of isotropic material in biomechanical studies of the glenoid, particularly in FE model development. The degree of anisotropy is generally larger in the posterior than in the anterior or central regions. This matches the results obtained for the apparent density, compressive strength, and elastic modulus. The degree of anisotropy is higher in the lateral region of the glenoid than in the medial region, which implies that the lateral region of the glenoid is more sensitive to loading conditions than is the medial region.

The trabecular architecture of the glenoid generally shows that the trabeculae in the glenoid are primarily aligned perpendicular to the glenoid articular surface. The trabeculae in the posterior portion and bare region are more effectively aligned to bear forces normal to the glenoid articular surface. These findings suggest that the glenoid is primarily subjected to higher loads in the posterior and bare regions. The compressive strength, elastic modulus, and elastic tensors in the posterior portion of the bare region of the glenoid were consistently 1.5 times the values in the other regions. This agrees with the characteristics of the trabecular architecture described above. Likewise, the trabeculae are inclined slightly anteriorly (average predominant trabecular direction: 91.1 ± 8.8°) in the lateral region of the glenoid (refer

to Fig. 6). This confirms that the posterior area is loaded more intensely than the anterior or central regions. All these results concur with the regional variations reported for the material properties, such as bone density or strength [27-30], and the mechanical characteristics, such as loading conditions on the glenoid [34, 13, 22]. This suggests that an analysis of the morphological and mechanical characteristics of the trabecular bone would help to predict the predominant loading placed on the glenoid.

The material investigated in this study was from the cadavers of normal elderly adults, owing to the limited availability of cadaver specimens. In the future, this study will be expanded to include pathological conditions and various age groups. The results may be used to explain the morphological and mechanical characteristics of the glenoid with musculoskeletal pathology and the consequent variation in the predominant loading condition on the glenoid. This study was innovative in its detailed mapping of the morphological and material characteristics of the glenoid and its pioneering approach used to estimate the loading pattern acting on the glenoid through the relationship between the mechanics and the morphology and material. The results obtained here may also be used to understand a variety of pathological shoulder conditions and may be applicable to related orthopedic implants and therapies.

Acknowledgment

This work was supported by the Korea Science and Engineering Foundation (KOSEF) grant funded by the Korea government(MEST) (NO. R01-2008-000-11641-0) and supported in part by the Calhoun Fellowship Fund of the School of Biomedical Engineering, Science and Health Systems, of Drexel University. The help provided by the Departments of Orthopedics and Radiology at the Drexel Medical School is gratefully acknowledged.

References

[1] E. J. Cheal, B. D. Snyder, D. M. Nunamaker and W. C. Hayes, Trabecular bone remodeling around smooth and porous implants in an equine patellar model, *Journal of Biomechanics*, 20 (1987) 1121.

[2] S. C. Cowin, The relationship between the elasticity tensor and the fabric tensor, *Mechanics Materials*, 4 (1985) 137-147.

[3] S. C. Cowin, Bone mechanics handbook, CRC Press LLC, Boca Raton, FL (2001).

[4] L. A. Feldkamp, S. A. Goldstein, M. Parfitt, G. Jesion and M. Kleerekoper, The direct examination of three-dimensional bone architecture in vitro by computed tomography, *Journal of Bone and Mineral Research*, 4 (1989) 3-11.

[5] S. A. Goldstein, L. S. Matthews, J. L. Kuhn and S. J. Hollister, Trabecular bone remodeling: an experimental model, *Journal of Biomechanics*, 24 (Suppl. 1) (1991) 135-150.

[6] R. E. Guldberg, M. Richards, N. J. Caldwell, C. L. Kuelske and S. A. Goldstein, 1997., 30, 147, Trabecular bone adaptation to variations in porous-coated implant topology, *Journal of Biomechanics*, 30 (1997) 147-153.

[7] T. P. Harrigan and R. W. Mann, Characterization of microstructural anisotropy in orthotropic material using a second rank tensor, *Journal of Materials Science*, 19 (1984) 761-767.

[8] R. Huiskes, R. Ruimerman, G. H. van Lenthe and J. D. Janssen, Effect of mechanical forces on maintenance and adaptation of form in trabecular bone, *Nature* 405 (2000) 704-706.

[9] J. Kabel, B. van Rietbergen, A. Odgaard and R. Huiskes, Constitutive relationship of fabric, density, and elastic properties in cancellous bone architecture, *Bone* 25 (1999) 481-486.

[10] Z. Miller, M. B. Fuchs and A. M., Trabecular bone adaptation with an orthotropic material model, *Journal of Biomechanics* 35 (2002) 247-256.

[11] D. C. Newitt, S. Majumdar, B. van Rietbergen, G. von Ingersleben, S. T. Harris, H. K. Genant, C. Chesnut, P. Garnero and B. MacDonald, In vivo assessment of architecture and micro-finite element analysis derived indices of mechanical properties of trabecular bone in the radius, *Osteoporosis International*, 13 (2002) 6-17.

[12] A. Odgaard, Three-dimensional methods for quantification of cancellous bone architecture, *Bone* 20 (1997) 315-328.

[13] A. Odgaard, E. B. Jensen and J. G. Gundersen, Estimation of structural anisotropy based on volume orientation: A new concept, *Journal of Microscopy*, 157 (1990) 149-162.

[14] A. Odgaard, J. Kabel, B. van Rietbergen, M. Dalstra and R. Huiskes, Fabric and elastic principal directions of cancellous bone are closely related, *Journal of Biomechanics*, 30 (1997) 487-495.

[15] S. R. Simon, Orthopaedic basic science, American

Academy of Orthopaedic Surgeons, (1994).
[16] K. Tsubota, T. Adachi and Y. Tomita, Functional adaptation of cancellous bone in human proximal femur predicted by trabecular surface remodeling simulation toward uniform stress state, *Journal of Biomechanics*, 35 (2002) 1541-1551.
[17] C. H. Turner and S. C. Cowin, Dependence of the elastic constants of an anisotropic porous material upon porosity and fabric, *Journal of Materials Science*, 22 (1987) 3178-3184.
[18] C. H. Turner, S. C. Cowin, J. Y. Rho, R. B. Ashman and J. Rice, The fabric dependence of the orthotropic elastic constants of cancellous bone, *Journal of Biomechanics*, 23 (1990) 549-561.
[19] G. H. van Lenthe and R. Huiskes, How morphology predicts mechanical properties of trabecular structures depends on intra-specimen trabecular thickness variations, *Journal of Biomechanics*, 35 (2002) 1191-1197.
[20] B. van Rietbergen, R. Muller, D. Ulrich, P. Ruegsegger and R. Huiskes, Tissue stresses and strain in trabeculae of a canine proximal femur can be quantified from computer reconstructions, *Journal of Biomechanics*, 32 (1999) 165-173.
[21] B. van Rietbergen, A. Odgaard, J. Kabel and R. Huiskes, Direct mechanics assessment of elastic symmetries and properties of trabecular bone architecture: Technical note, *Journal of Biomechanics*, 29 (1996) 1653-1657.
[22] B. van Rietbergen, A. Odgaard, J. Kabel and R. Huiskes, Relationships between bone morphology and bone elastic properties can be accurately quantified using high-resolution computer reconstructions, *Journal of Orthopaedic Research*, 16 (1998) 23-38.
[23] W. J. Whitehouse, The quantitative morphology of anisotropic trabecular bone, *Journal of Microscopy*, 101 (1974) 153-168.
[24] G. H. von Meyer, Die architektur der spongiosa, *Arch. Anat. Physiol. Wiss. Med.*, 34 (1867) 615-628.
[25] J. Wolff, Thelaw of bone remodeling, Springer, Berlin, (1986).
[26] S. C. Cowin, Bone mechanics handbook, CRC Press LLC, Boca Raton, FL (2001).
[27] C. Anglin, P. Tolhurst, U. P. Wyss and D.R. Pichora, Glenoid cancellous bone strength and modulus, *Journal of Biomechanics*, 32 (1999) 1091-1098.
[28] L. H. Frich, N. C. Jensen, A. Odgaard, C. M. Pedersen, J. O. Sjbjerg and M. Dalstra, Bone strength and material properties of the glenoid, *Journal of Shoulder and Elbow Surgery*, 6 (1997) 97-104.
[29] L.H. Frich, A. Odgaard and M. Dalstra, Glenoid bone architecture, *Journal of Shoulder and Elbow Surgery*, 7 (1998) 356-361.
[30] P. Mansat, C. Barea, M. C. Hobatho, R. Darmana and M. Mansat, Anatomic variation of the mechanical properties of the glenoid, *Journal of Shoulder and Elbow Surgery*, 7 (1998) 109-115.
[31] P. K. Zysset, A review of morphology–elasticity relationships in human trabecular bone: theories and experiments, *Journal of Biomechanics*, 36 (2003) 1469-1485.
[32] L. J. Gibson and M. F. Ashby, The mechanics of three-dimensional cellular materials, *Proceedings of the Royal Society London A*, 382 (1982) 43-59.
[33] J. C. Wang, Young's modulus of porous materials *Journal of Materials Science*, 19 (1984) 801-808.
[34] C. Anglin, U. P. Wyss and D. R. Pichora, Glenohumeral contact forces, *Proceedings of the Institution of Mechanical Engineers*, 214 (2000) 637-644.

Dohyung Lim received B.S. and M.S. degrees in Biomedical Engineering from Inje University, Kimhae, Korea, in 1998 and 2000, respectively. He then went on to receive his Ph.D. degree from School of Biomedical Engineering, Science, & Health Systems, Drexel University, Philadelphia, PA, USA, in 2004. Dr. Lim completed a postdoctoral fellowship in Department of Physical Therapy and Human Movement Science, Feinberg School of Medicine, Northwestern University, Chicago, IL, USA and a Research Professor of Biomedical Engineering, Yonsei University, Wonju, Gangwon, Korea. Dr. Lim is currently a Senior Researcher at the Korea Institute of Industrial Technology in Cheonan, Chungnam, Korea.

Han-Sung Kim received B.S. and M.S. degrees in Machine Design and Production Engineering from Hanyang University, Seoul, Korea, in 1989 and 1991, respectively. Dr. Kim received Ph.D. degree in Mechanical Engineering from University of Manchester Institute of Science and Technology, Manchester, UK, in 1999. Dr. Kim is currently an Associated Professor at the Biomedical Engineering at Yonsei University in Wonju, Korea.

Jung-Sung Kim received B.S. and M.S. degrees in Biomedical Engineering from Inje University, Kimhae, Korea, in 1996 and 1998, respectively. He is currently in the doctor's course in Department of Medical Engineering and BK 21 Project for Medical Science, Yonsei University College of Medicine, Seoul, Korea.

Rami Seliktar has a BS and MS degree in Mechanical Engineering, from The Technion, IIT, and Ph.D. (BME) from Strathclyde University, Scotland. He has held academic appointments in several institutions worldwide: Strathclyde University (2yrs.); associate professor at the Technion (9yrs.); Texas A&M (on sabbatical leave from the Technion), and twenty seven years as professor of BME and ME at Drexel University in Philadelphia. Concurrently he founded and directed a Biomechanics laboratory at the Loewenstein Rehab. in Israel and consulted to governments, public agencies and industries. Prof. Seliktar has done research on limb prosthetics, human performance, orthopedic and occupational biomechanics, assistive technology for automomobil dynamics. His research has been funded by: The NSF, NIH, the RWJ Foundation, the Easter Seal Foundation, NIDRR, AIduPont, the United Cerebral Palsy and some hospitals. He has published numerous articles in scientific journals, book chapters and conference proceedings. At the present, Rami Seliktar is Professor and Vice Director of the School of Biomedical Engineering, Science and Health Systems of Drexel University.

Sung-Jae Lee received B.S. and M.Eng. degrees in Mechanical Engineering from Cornell University, Ithaca, NY, USA, in 1984 and 1985, respectively. He re-ceived Ph.D. degree in Biomedical Engineering from University of Iowa, Iowa City, IA, USA, in 1993 Dr. Lee is currently a Professor at Department of Biomedical Engineering, Inje University, Gimhae, Gyongnam, Korea. He is currently serving as a board member for the Division for Health Care Technology Assessment of International Federation of Medical and Biological Engineering (IFMBE), a executive member of Korean Orthopedic Research Society, director of international relations for the Korean Society for Biomaterials and also for the Korean Society of Biomechanics.